Modeling and assessing adaptive cruise control stability: experimental insights

Raphael Stern
Dept. of Civil, Environ., and Geo- Eng.
University of Minnesota
Minneapolis, USA
Dept. of Informatics, Tech. Univ. Munich
Munich, Germany
rstern@umn.edu

George Gunter
Dept. of Civil and Environ. Eng.
University of Illinois
Urbana, USA
gunter1@illinois.edu

Daniel B. Work
Inst. for Software Integrated Systems
Dept. of Civil and Environ. Eng.
Vanderbilt University
Nashville, USA
dan.work@vanderbilt.edu

***Abstract*—Adaptive cruise control is a first step towards increasingly automated vehicles, and while ACC offers potential benefits to the traffic stream depending on the ACC design, less is known about the impacts that commercially available ACC vehicles have traffic flow. Therefore, it is of interest to reliably model commercial ACC vehicle behavior so as to be able to better understand how ACC vehicles may influence the emergent properties of the traffic flow. In this article, a set of car following experiments are conducted to collect data from a 2015 fully electric sedan equipped with a commercial adaptive cruise control system. Velocity, relative velocity, and space gap data collected during the experiments are used to calibrate two dynamical models for the ACC vehicle, one for each of two following settings. The models are calibrated via model-constrained optimization. The main finding is that the best fit models are unstable. To better understand how much the quality of the models would have to change to alter their stability, we calibrate the models with the constraint that they must be string stable and compare both the new model error as well as the calibrated parameter values. We find that the quality of fit for the minimum following setting degrades by 26%, while the quality of fit for the maximum following setting model only degrades by 7%, but requires significant changes in the parameter values.**

***Index Terms*—Adaptive cruise control; phantom traffic jams; field experiments; traffic modeling.**

I. Introduction

Autonomous vehicles (AVs) have captured the interest of researchers over the past several years. However, not all AVs are the same in terms of the autonomous capabilities they possess. Specifically, the *Society of Automotive Engineers* (SAE) has defined six levels of *automated driving systems* (ADSs) that define different degrees of automation [1]. These levels range from no automation (Level 0) through full automation (Level 5), with increasing autonomy from Level 0 through Level 5.

The first ADSs that will become prevalent in the traffic flow are Level 1 and 2 vehicles with driver assist features such as *adaptive cruise control* (ACC) [2]. These features were historically considered premium features on luxury vehicles, but are now becoming commonplace on many commercially available vehicles. For example, 16 of the 20 best-selling vehicles in the US in 2018 were available with ACC as a standard or optional feature [3]. Therefore, the impact that commercial ACC vehicles will have on traffic flow is of particular relevance.

While some traffic jams arise from bottlenecks in the road, other traffic jams arise as an emergent property of human driving behavior [4]. The latter types of traffic jams are often referred to as *phantom jams* since they seemingly arise for no clear reason. However, as was show in the experimental work by Sugiyama, et al. [4] and Tadaki, et al. [5] and verified by Wu, et al. [6], [7], these phantom jams are a result of human driving behavior alone, which is sufficient to trigger stop-and-go waves. In these experiments, a large circular track was used with human-piloted vehicles that started with a uniform initial space gap and at the same speed. The circular ring road setup was used since it represents infinite traffic where every vehicle has a vehicle in front of it (a lead vehicle) and a vehicle behind it. Due to the human driving behavior, this initial uniform traffic quickly devolves into stop-and-go waves. Such behavior is a result of *string unstable* car following dynamics since small perturbations from the initial equilibrium flow (all vehicles at the same speed and space gap with no acceleration) amplify as they propagate from one vehicle to the next back in the traffic stream [8].

To model traffic flow that exhibits such instabilities, a variety of models have been proposed. Specifically, models that describe traffic dynamics at the level of the individual vehicle are referred to as *microscopic* models, and frequently use an *ordinary differential equation* (ODE) to model the dynamics of an individual vehicle as a response to the vehicle's surroundings. These models have been popular since the 1950s when early experimental work by researchers at General Motors collected vehicle speed and space gap data to describe human driving behavior [9]–[13]. Since then, many popular models have been proposed and become prevalent in the research literature, including the *Gipps model* [9], the *intelligent driver model* [14], and the *optimal velocity model* [15].

This material is based upon work supported by the National Science Foundation under Grants No. CNS-1837652 (D.W. & R.S.) and OISE-1743772 (G.G.) as well as through the Federal Highway Administration's Dwight David Eisenhower Transportation Fellowship Program under Grant No. 693JJ31845050 (R.S.).

It has been shown that AVs are capable of stabilizing traffic flow and preventing phantom traffic waves from arising [16]. This has been studied in theory [17] and experimentally. In the experimental work by Stern, et al. [18], a setup similar to that in the ring-road experiments described above [4]–[7] was used with the difference that one vehicle was an autonomous capable vehicle. This vehicle was used to control the traffic flow. The result was that a single AV out of 21 vehicles was able to stabilize the traffic flow. The stabilizing controller reduced fuel consumption by 39%, reduced emissions by up to 74%, and increased the throughput of the road by up to 14% when comparing the oscillatory traffic without an AV to the stabilized traffic flow when the AV was actively dampening the traffic waves [16], [18]. Importantly, these results were achieved with only one in 21 vehicles (roughly 5% of the overall flow) driving autonomously while the remaining vehicles were all human piloted.

Other research efforts have focused on the use of *cooperative adaptive cruise control* (CACC) vehicles to achieve string stable traffic by forming platoons of CACC vehicles. In such a scheme, all vehicles in the platoon use the same automation technology and *vehicle to vehicle* (V2V) communication to achieve string stability. Notably, the use of connectivity for platoons of ACC vehicles has been explored both theoretically [19]–[23] and through several experiments and demonstrations [24]–[27]. Many of the significant developments in vehicle automation including platooning were created from USDOT Automated Highway System program, see [28] for an overview.

These previous works highlight that even just a small number of vehicles driving in a way that is distinct from the remaining traffic flow may substantially alter the emergent properties of the flow. Therefore, there is substantial interest in modeling the vehicle-level dynamics of ACC vehicles to understand how they may interact with human piloted vehicles, and how they may influence traffic string stability [29], [30].

The impact that ACC vehicles without connectivity have on traffic flow and traffic stability has also been an area of interest in the research community. Simulation-based studies, for example by Davis [31], [32], have shown that ACC vehicles may be able to stabilize the traffic flow at a market penetration rate as low as 20%. However, only a few works have experimentally studied the string stability properties of commercially available ACC vehicles. Notably, Milanés et al. [29] instrumented commercially available ACC vehicles and found that the vehicle make and model tested was string unstable.

While commercially implemented ACC systems must meet a number of design criteria including vehicle safety and rider comfort, they may currently not be optimized considering their impacts on overall traffic flow. However, as has been shown before, changing the dynamics of only a small number of agents in the traffic flow may be sufficient to change the emergent properties of the flow and substantially change the traffic characteristics [16]. Therefore, there is significant interest in being able to accurately and reliably model the vehicle-level behavior of ACC systems in a way in which they can be analyzed to understand their impacts on the traffic flow, in line with earlier investigations [17], [21], [31], [33]–[37] of experimental vehicles and simulation studies.

With that in mind, the goal of this article is to determine the string stability of a commercially available adaptive cruise control system, and analyze the sensitivity of the model parameter values and model accuracy to the requirement for the model to be string stable or string unstable. An extended version of the experimental setup, model calibration, and stability analysis is available in [38] (ArXiv preprint available at [39]), which provides more detail on the experimental setup and the stability analysis conducted. The new contribution beyond [39] is to conduct a sensitivity analysis on the stability of the calibrated model to understand how much the modeling error must be increased by to obtain the best-fit model that changes the string stability result. We find that a 26% increase in training error is required to change the best fit model from string unstable to string stable when operating at the minimum following setting, while a 7% increase in training error is required to change the corresponding maximum following setting model from string unstable to string stable. For both following settings, the model parameter values must change substantially to achieve string stability.

The remainder of this article is outlined as follows: in Section II the vehicle-level ACC model is introduced and a method for analyzing the its string stability is introduced. The experimental setup and test vehicle is described in Section III, and the calibration methodology is outlined in Section IV. The stability analysis is conducted in Section V, and it is illustrated that the stability results for the best fit models are not sensitive to small changes in the calibrated parameter values. The main findings are summarized in Section VI.

II. Modeling and Stability Analysis of ACC System

In this section, the ACC dynamical model and method of analyzing a model for string stability are reviewed. We begin by introducing a general framework for modeling ACC vehicles, then present the specific model that will be used in this article. The model is a simplified ACC model that has been previously used in [29], [40]. Next, we review method to assess the string stability of an ACC model.

A. General ACC model

When modeling an ACC vehicle, there are many factors that influence the vehicle dynamics. These factors may include engine RPM, engine temperature, and road grade among others [41]. However, for the purpose of modeling the vehicle-level behavior in the traffic flow, this simulation granularity may not be necessary, or even desired.Instead, the focus of this work is to construct a high-level model of the ACC vehicle as a whole, and model how the ACC vehicle responds just to its traffic state.

Specifically, in this article, we model the response of an ACC vehicle to a lead vehicle immediately in front of it. We assume that through the on-board sensors, the ACC vehicle is able to measure the space gap between the lead vehicle and the ACC vehicle, s, as well as its own speed v and the relative speed with respect to the lead vehicle Δv. Using these inputs, the acceleration of the ACC vehicle $\ddot{x}(t)$ is modeled as an ordinary differential equation with the general form:

$$\ddot{x}(t) = f(s, v, \Delta v), \tag{1}$$

where s is the space gap, $v = \dot{x}(t)$ is the velocity of the follower, and $\Delta v := \dot{s}(t)$ is the relative velocity between the leader and follower.

When selecting parameter values for such a car following model, it is desirable that the model satisfy the *rational driving constraints* (RDC) [8]:

$$\frac{\partial f}{\partial s} := f_s \geq 0, \tag{2}$$

$$\frac{\partial f}{\partial \Delta v} := f_{\Delta v} \geq 0, \tag{3}$$

$$\frac{\partial f}{\partial v} := f_v \leq 0. \tag{4}$$

Roughly speaking, the rational driving constraints ensure that the following vehicle behaves as a rational driver would. I.e., the following vehicle will drive faster when space gap increases or the lead vehicle increases its speed, and will begin to slow as it reaches the maximum desirable speed.

B. OVRV model

One model which has previously been used to model ACC vehicle dynamics is the *optimal velocity* model with a *relative velocity* term (OVRV), which together takes the form:

$$\ddot{x}(t) = \alpha \left(V(s) - v \right) + \beta \left(\Delta v \right). \tag{5}$$

In the above model (5), the first component relaxes the follower velocity to a desired velocity prescribed by the *optimal velocity* function V based on the current space gap to the vehicle in front, while the second component relaxes the follower velocity to the velocity of the leader. The parameters α and β control the tradeoffs between following the optimal velocity and following the leader velocity.

For the purposes of modeling ACC vehicles, we adopt a special case of the OVRV model (5) considered in [30], [32], [40]:

$$\ddot{x} = f(s, v, \Delta v) = k_1(s - \eta - \tau_e v) + k_2(\Delta v) \tag{6}$$

where k_1 and k_2 are the gain parameters on the optimal velocity term and a follow-the-leader term respectively, η is the jam space gap (the minimum distance two vehicles will attain) and the parameter τ_e is the desired headway. Note that the model (6) corresponds to a linear optimal velocity function $V(s) := s/\tau_e$ and with $\alpha := k_1 \tau_e$. The model (6) is selected based on the reported goodness of fit to simulate real trajectories of ACC equipped vehicles in [30], [40].

C. Stability analysis

String stability tells whether small disturbances from equilibrium space gap will amplify or dissipate as they propagate from one vehicle to the next in a platoon. Therefore, string stability is critical for understanding whether phantom jams will form, or whether small disturbances will be dissipated through the traffic flow. To analyze a car following model for string stability, we follow the common procedure outlined by Wilson and Ward [8].

Specifically, the string stability of the following model which satisfies the RDC is considered:

$$\begin{aligned} \dot{s}(t) &= \Delta v \\ \dot{v}(t) &= f(s, v, \Delta v) + d, \end{aligned} \tag{7}$$

where d represents a disturbance to the acceleration. A straightforward criterion for string stability that relies only on the partial derivatives of the car following model is presented by Wilson and Ward [8]:

$$\lambda_2 := \frac{f_s}{f_v^3} \left[\frac{f_v^2}{2} - f_{\Delta v} f_v - f_s \right] < 0. \tag{8}$$

In the case of the model 5, this can easily be evaluated for a particular set of calibrated model parameter values since $f_s = k_1$, $f_v = -k_1 \tau_e$, and $f_{\Delta v} = k_2$.

To illustrate the string stability of the model (5), we show the parameter space and corresponding stability result (stable vs. unstable) in Figure 1. As can be seen in the figure, increasing k_1, k_2 or τ_e all drive the model toward string stability. However, increasing k_1 and k_2 may not be feasible within the physical constraints on the vehicle dynamics, while increasing τ_e is generally always possible yet may not always be desirable since it may result in a lower roadway throughput. Additionally, note that the value of η does not influence the string stability of the model.

III. Experimental Overview and Test Vehicle Description

In this section we present the design and execution of a of field experiment to collect ACC car following data. A brief summary of the data collection methods are provided in this article, with a more complete description available in [39].

The goal of the experiment is to observe the vehicle following dynamics of an ACC-equipped vehicle. Each experiment involves a lead vehicle that executes a pre-determined velocity profile and a following vehicle that follows the lead vehicle under adaptive cruise control.

The test (following) vehicle is a commercially-available 2015 model-year fully electric luxury sedan. The ACC system in the test vehicle has two input settings: desired speed and desired following setting (ranging from close to far as selected by the driver). The desired speed is set by the driver, and can be specified to the nearest mile per hour. In the tests conducted in this work, only the minimum and maximum following setting are considered out of the possible options.

Each vehicle is equipped with a *U-blox EVK-M8T* GPS evaluation kit that is capable of tracking the position and speed

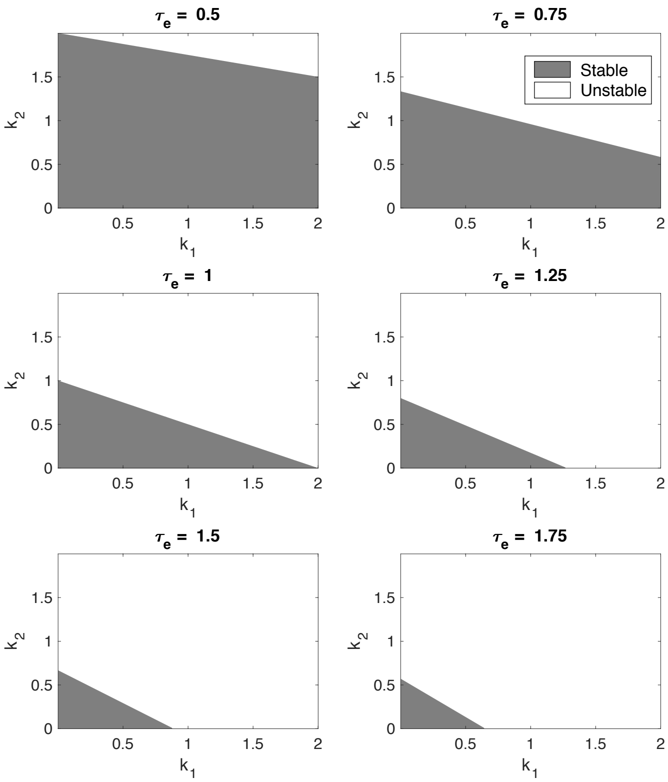

Fig. 1. Model stability for a range of gain values k_1 and k_2. The model is string stable for $\lambda_2 < 0$, indicated in grey. This demonstrates that the model can be calibrated to be either string stable or string unstable depending on the selected parameter values. Note that the value of η does not influence string stability.

of each vehicle throughout the experiment at a frequency of up to 10 Hz. Each evaluation kit is connected to a *Raspberry Pi* computer, which runs a script to log the data as it is recorded. While GPS is prone to small errors in position, these are often due to atmospheric conditions and are generally correlated for different GPS receivers in the same proximity.

During the test, the vehicles are arranged with the lead vehicle in front under human control, while the following vehicle operates under control of the ACC system as seen in Figure 2. The test is designed to capture a range of vehicle following speeds and transitions between these speeds. A total of nine different lead vehicle speed profiles are tested, and data for each speed profile are recorded for the following vehicle both at the minimum and at the maximum following setting. Thus, in total, 18 tests are conducted. The tests span a range of speeds from 5 mph (2.2 m/s) to 70 mph (31.3 m/s) and include portions of constant speed driving as well as portions of driving with rapid changes in the lead vehicle's speed. A full description of the tests in presented in the extended manuscript [39].

The test that is used for illustrative purposes in this article is the medium-velocity 5 mph oscillations test. In this test, the lead vehicle begins at 50 mph (22.4 m/s) and holds this speed for 30 seconds before reducing its speed to 45 mph (20.1 m/s), and holds this speed for 30 seconds before returning to 50 mph. This oscillatory driving is repeated until the test is over. An example of the oscillatory driving pattern is seen in the results in Figure 3 and Figure 4.

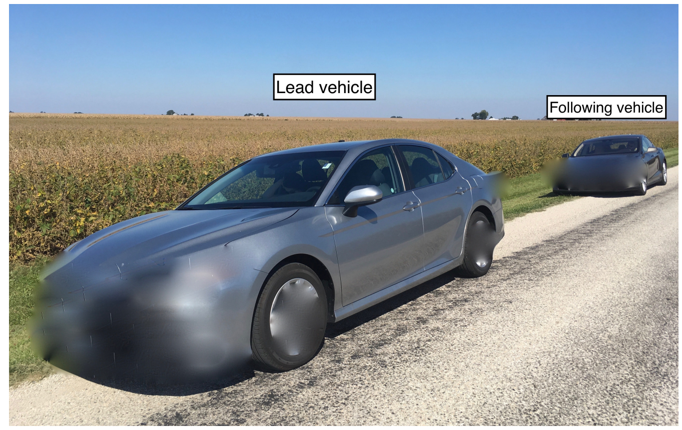

Fig. 2. Two-vehicle experimental setup in car following experiments with lead vehicle under human control and following vehicle under ACC control. Note that the identifying features of the lead vehicle and following vehicle have been masked to maintain anonymity of the vehicle being tested.

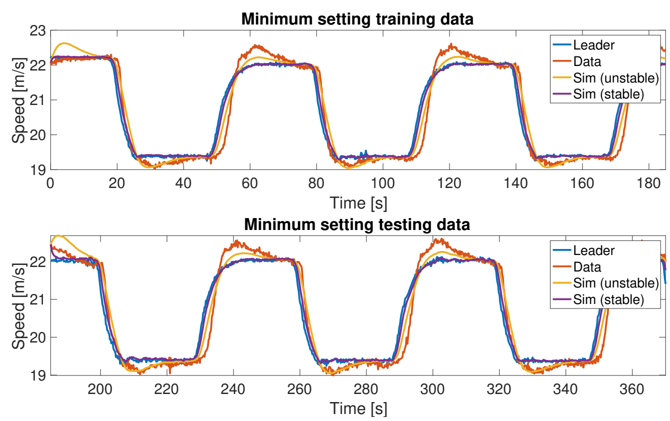

Fig. 3. Plot showing the actual lead vehicle and following vehicle speed as well as the simulated speeds using model that is calibrated to be unstable and the model that is calibrated to be string stable for the minimum following setting. The top plot shows the performance on the training data, while the bottom plot shows the performance on the testing data.

IV. Model Calibration Methodology

In order to calibrate an ACC dynamical model, the model parameters must be estimated from the data. The calibration of the model can be posed as a simulation-based optimization problem in which an error functional is minimized by selecting optimal model parameters. In Milanés and Shladover [29] an absolute valued error metric is proposed that compares the velocity of the ACC model under a given set of parameters to the velocity recorded by the real ACC equipped vehicle. In this work, the *root mean square error* (RMSE) is used due to its demonstrated good performance for the vehicle being tested. The RMSE is computed as follows:

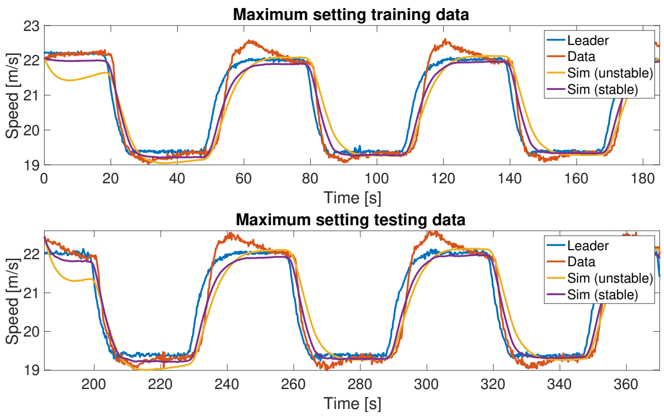

Fig. 4. Plot showing the actual lead vehicle and following vehicle speed as well as the simulated speeds using model that is calibrated to be unstable and the model that is calibrated to be string stable for the maximum following setting. The top plot shows the performance on the training data, while the bottom plot shows the performance on the testing data.

$$\text{RMSE} = \sqrt{\frac{1}{T}\int_0^T (v_\text{m}(t) - v(t))^2 dt}. \tag{9}$$

In (9) the term $v(t)$ is the simulated velocity of the following vehicle at time t, $v_\text{m}(t)$ is the measured velocity of the following vehicle in the data at time t, and T is the duration of the data collection period. Practically, in implementation, the RMSE is computed at the discrete time steps when measurements are collected (10 Hz).

The optimal parameters are found by solving a constrained optimization problem where the objective function is the speed RMSE between simulation with the optimal parameter values and the collected data. The problem is constrained to satisfy the RDC. Furthermore, for each following setting (maximum and minimum) the calibration is done twice: once with the model being unconstrained with respect to string stability, where the model is found to be string unstable, and once with the model constrained to string stable parameter values. This allows for comparison between the quality of fit between the string stable model and the string unstable model, and provides a sensitivity analysis on the quality of fit of the stability finding.

The task of finding the optimal parameter values k_1, k_2, τ_e, and η thus relies on solving the following optimization problem:

$$\begin{aligned}
\underset{s,v,k_1,k_2,\tau_e,\eta}{\text{minimize}} \ : \quad & \sqrt{\tfrac{1}{T}\textstyle\int_0^T (v_\text{m}(t) - v(t))^2 dt} \\
\text{subject to:} \quad & \dot{v}(t) = f(s, v, \Delta v) \\
& \dot{s}(t) = v_{\ell,\text{m}}(t) - v(t) \\
& s(0) = s_\text{m}(0) \\
& v(0) = v_\text{m}(0) \\
& k_1 \geq 0 \\
& k_2 \geq 0 \\
& \tau_e \geq 0 \\
& \eta \geq 0,
\end{aligned} \tag{10}$$

to calibrate the string unstable model and:

$$\begin{aligned}
\underset{s,v,k_1,k_2,\tau_e,\eta}{\text{minimize}} \ : \quad & \sqrt{\tfrac{1}{T}\textstyle\int_0^T (v_\text{m}(t) - v(t))^2 dt} \\
\text{subject to:} \quad & \dot{v}(t) = f(s, v, \Delta v) \\
& \dot{s}(t) = v_{\ell,\text{m}}(t) - v(t) \\
& s(0) = s_\text{m}(0) \\
& v(0) = v_\text{m}(0) \\
& k_1 \geq 0 \\
& k_2 \geq 0 \\
& \tau_e \geq 0 \\
& \eta \geq 0 \\
& \tfrac{k_1}{-k_1^3\tau_e^3}\left[\tfrac{k_1^2\tau_e^2}{2} + k_1 k_2 \tau_e - k_1\right] \leq 0,
\end{aligned} \tag{11}$$

to calibrate the string stable model. In (10) and (11), $v_{\ell,\text{m}}(t)$ is the measured velocity of the lead vehicle. In both optimization problem formulations the last constraint enforces the desired stability result.

The optimal parameter values are found using an constrained quasi-Newton search method as implemented in the `fmincon` function in Matlab. The simulation of the follower vehicle trajectory at each step of the optimization routine is performed via numerical integration using an explicit forward Euler scheme. Because the resulting optimization problem is nonlinear and to account for potential local minima, the optimization routine is run many times using randomly initialized parameters. The parameter value set that yields the lowest RMSE is selected as the best fitting parameters. The results of this approach is presented in the next section.

Data from all speed profiles is used during calibration. Specifically, each test is divided in two with the first half being used as training data, and the second half being used as testing data. The model is calibrated by combining all the training data.

V. Results

In this section we first provide an analysis of the accuracy of the GPS units that are used to measure vehicle positions and speeds. Next the calibration of the dynamical model outlined in (6) is presented, and the results are compared to the measured ACC data. The change in the parameters and the overall model quality of fit required to make the model string stable (compared to string unstable, which is the best fitting model), is discussed.

A. Validation of GPS measurements

The U-blox evaluation kits are tested for accuracy in speed and position by placing two U-blox sensors a known distance apart on the same vehicle and extensively driving this vehicle to observe the GPS measured distance and difference in speed throughout the drive.

The distance between the two antennae mounted on the same vehicle is computed using the Haversine formula. The mean recorded sensor distance is 1.37 m compared to an actual sensor distance of 0.94 m. This corresponds to a mean position accuracy accuracy of 0.43 m, which translates to roughly 1% error when compared to the following distances observed in the experiments. The mean absolute difference in speed between the two sensors is 0.06 m/s (0.13 mph), which is an error of less than 0.2% of the average speeds observed in the tests.

Due to the overall good agreement between sensor speed and position measurements, the U-blox EVK-M8T is a suitable GPS unit for recording velocity and position data.

B. Model calibration and sensitivity analysis

In this section, the calibration results for both the model that is unconstrained with respect to string stability as well as the model that is calibrated with respect to string stability are discussed. The quality of fit of each of these models for both following settings is compared.

The calibrated model parameter values and corresponding training error are presented in Table I. For both the maximum following setting and the minimum following setting the best fit model is found to be string unstable when stability is not enforced. The percent increase in training error from the best-fit model to the string stable model simulated given k_1, k_2, and τ_2 is shown in Figure 5 for the minimum following setting. Recall that the value of η does not influence string stability of the model. For plotting purposes, the difference in training error is capped at 100% higher than the best-fit model training error. Thus, the yellow represents regions of the parameter space that produce a training error that is twice as high or higher as compared to the best fit model. This plot shows that the training error is highly sensitive to τ_e, since small changes in the value of τ_e greatly increase the training error.

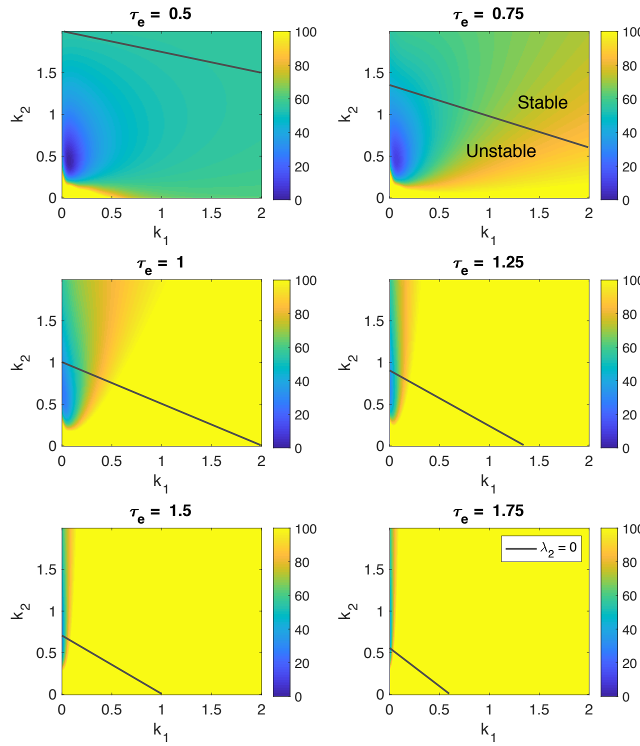

Fig. 5. Percent change from the best fit model to the model with given k_1, k_2, τ_e and $\eta = 8.34$ in Table I for the minimum following setting. The line $\lambda_2 = 0$ from Figure 1 is superimposed to show the stable and unstable parameter space. Recall from Figure 1 that parameters above the line $\lambda_2 = 0$ correspond a stable model in (5). Also note that for plotting purposes, the maximum percent increase displayed is 100%. However, greater percent increases are present. Thus, the error should be thought of as at least 100% greater increase between the best-fit model and the model with the given parameter values.

In Figure 6, the percent training errors from the overall best-fit model for the stable and unstable model are shown. The top plot shows that the best-fit (unconstrained with respect to stability) model has the lowest overall training error and lies in the unstable parameter space. However, when the model is constrained to be string stable, the training error increases by roughly 26% from the best-fit model and the resulting model is just above the line $\lambda_2 = 0$. I.e., the best-fit model that is constrained to be string stable has substantially higher training error. However, the corresponding plot for the maximum following setting in Figure 7 shows that the change in training error is comparatively small (7%) between the string unstable model and the string stable model.

Additionally, the model parameter values for both the maximum and the minimum following setting would have to change substantially for the model to become string stable. Specifically, a reduction of over 99% in the value of k_1 is required for both the minimum and maximum following setting, an increase in k_2 of 53.8% is require for the minimum following setting. However, an increase in k_2 of only 5.6% is required for the maximum following setting to become string stable. The main interpretation of these parameter changes is that the emphasis on the constant time headway term is reduced substantially compared to the relative velocity term when the models are constrained to be string stable. Moreover, when the model is constrained to string stable parameter values, the effective headway τ_e is increased (nearly three times as large for the minimum following setting and more than twice as large for the maximum following setting), and η is thus decreased by over 99% for both following settings. Recall though that the value of η does not influence string stability.

Finally, in Figure 3 the minimum following setting data is plotted along with the simulated speed profile using both the string unstable and string stable models. The plot shows that when the model is allowed to be string unstable, the model is capable of producing the same overshoots and undershoots as observed in the experimental data. However, when the model is constrained to be string stable, these overshoots are no longer compliant with string stability, and the model trajectories match the lead vehicle profile. Thus, the string stable model for the minimum following setting is effectively a follow-the-leader model and no longer captures the actual dynamics of the following vehicle. This behavior is observed in the training data as well as the testing data for the minimum following setting.

As seen in Figure 4 for the maximum following setting, the overshoot that the string unstable model produces does not

Following setting	Constraint	k_1 [1/s^2]	k_2 [1/s]	τ_e [s]	η [m]	Speed training error [m/s]	Speed testing error [m/s]	Spacing training error [m]	Spacing testing error [m]
minimum	unstable	0.0782	0.4445	0.5162	8.3365	0.23	0.22	1.51	1.37
minimum	stable	0.0002	0.6835	1.4634	0.0593	0.29	0.28	3.58	3.28
maximum	unstable	0.0131	0.2692	1.6881	7.5699	0.28	0.30	3.00	2.77
maximum	stable	0.0002	0.2843	3.5137	0.0090	0.30	0.32	6.85	5.65

TABLE I

CALIBRATED MODEL PARAMETER RESULTS FOR BOTH THE MODELS CONSTRAINED TO BE STRING STABLE AS WELL AS THE MODELS CONSTRAINED TO BE STRING UNSTABLE.

Following setting	Difference (%)					
	k_1	k_2	τ_e	η	Train error	Testing error
minimum	-99.7	53.8	183.5	-99.3	26.1	27.3
maximum	-98.5	5.6	108.1	-99.9	7.1	6.7

TABLE II

PERCENT CHANGE IN CALIBRATED PARAMETER VALUES BETWEEN MODEL CALIBRATED TO BE STRING STABLE AND MODEL CALIBRATED TO BE STRING UNSTABLE. THE BASELINE IS THE STRING UNSTABLE MODEL, WHICH HAD LOWEST TRAINING ERROR OVERALL. POSITIVE VALUES INDICATE THE CORRESPONDING PARAMETER VALUE FOR THE STRING UNSTABLE MODEL IS LARGER THAN THE CALIBRATED PARAMETER VALUE FOR THE STRING STABLE MODEL.

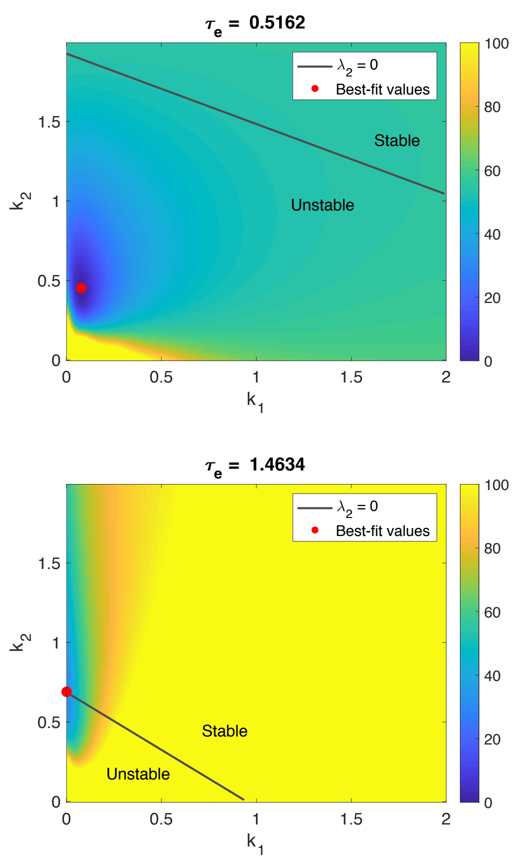

Fig. 6. Percent error from best-fit minimum following setting model for different parameter values evaluated at the τ_e of the unstable (top) and stable (bottom) best fit models. Note that the value of η does not influence the stability of the model. The best-fit parameters for each model are represented as a red dot.

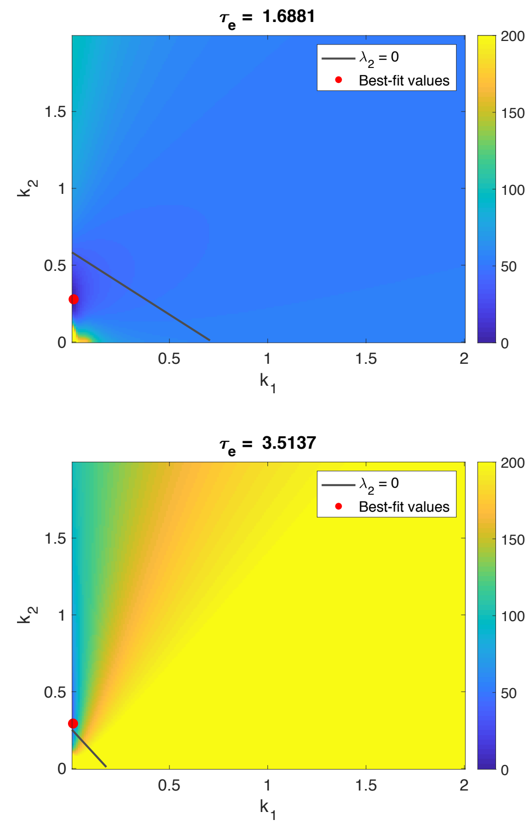

Fig. 7. Percent error from best-fit maximum following setting model for different parameter values evaluated at the τ_e of the unstable (top) and stable (bottom) best fit models. Note that the value of η does not influence the stability of the model. The best-fit parameters for each model are represented as a red dot. Note that for plotting purposes, the maximum percent increase in training error is 200% higher than the overall best fit model, all errors higher than this are displayed in yellow.

match the observed overshoot in the data. However, importantly the string unstable model matches the speed undershoot below the minimum speed that the lead vehicle brakes to observed in the data. Similarly to the minimum following setting, the string stable model for the maximum following setting becomes a follow the leader model and does not exhibit any overshoot or undershoot.

VI. CONCLUSIONS

In conclusion, the main finding of this article is that the tested vehicle is string unstable for both the minimum and maximum following setting, and that the results are robust. To assess the sensitivity of the finding, we add a constraint to the calibration routine requiring the resulting model to be string stable. With the additional requirement, we find that the quality of fit for the minimum following setting degrades by 26%, while the quality of fit for the maximum following setting model only degrades by 7%. However, for both the maximum and minimum following settings, the model parameter values would have to change substantially for the model to become string stable.

VII. Acknowledgements

The authors would also like to acknowledge Caroline Janssen, Yanbing Wang, Derek Gloudemans, William Barbour, Hannah Burson, and David Bergvelt for their assistance in data collection as well as Dr. Carl Gunter for providing the experimental vehicle.

References

[1] Society of Automotive Engineers. J3016: Taxonomy and Definitions for Terms Related to Driving Automation Systems for On-Road Motor Vehicles. Standard, June 2018.

[2] P. Bansal and K. M. Kockelman. Forecasting Americans' long-term adoption of connected and autonomous vehicle technologies. *Transportation Research Part A: Policy and Practice*, 95:49–63, 2017.

[3] Reuters. Top 20 vehicles sold in U.S. in April, May 2018.

[4] Y. Sugiyama, M. Fukui, M. Kikuchi, K. Hasebe, A. Nakayama, K. Nishinari, S. i. Tadaki, and S. Yukawa. Traffic jams without bottlenecks – experimental evidence for the physical mechanism of the formation of a jam. *New Journal of Physics*, 10(3):033001, 2008.

[5] S. Tadaki, M. Kikuchi, M. Fukui, A. Nakayama, K. Nishinari, A. Shibata, Y. Sugiyama, T. Yosida, and S. Yukawa. Phase transition in traffic jam experiment on a circuit. *New Journal of Physics*, 15:103034, 2013.

[6] F. Wu, R. Stern, S. Cui, M. L. Delle Monache, R. Bhadani, M. Bunting, M. Churchill, N. Hamilton, R. Haulcy, H. Pohlmann, B. Piccoli, B. Seibold, J. Sprinkle, and D. B. Work. Tracking vehicle trajectories and fuel rates in oscillatory traffic. *Transportation Research Part C: Emerging Technologies*, 88:82–109, 2019.

[7] F. Wu, R. E. Stern, M. Churchill, M. L. Delle Monache, K. Han, B. Piccoli, and D. Work. Measuring trajectories and fuel consumption in oscillatory traffic: Experimental results. In *Proceedings of the* 96^{th} *Transportation Research Board Annual Meeting*, 2017.

[8] R. E. Wilson and J. A. Ward. Car-following models: fifty years of linear stability analysis–a mathematical perspective. *Transportation Planning and Technology*, 34(1):3–18, 2011.

[9] P. G. Gipps. A behavioural car-following model for computer simulation. *Transportation Research Part B: Methodological*, 15(2):105–111, 1981.

[10] R. E. Chandler, R. Herman, and E. W. Montroll. Traffic dynamics: studies in car following. *Operations Research*, 6(2):165–184, 1958.

[11] R. Herman and R. B. Potts. Single lane traffic theory and experiment. 1959.

[12] R. Rothery, R. Silver, R. Herman, and C. Torner. Analysis of experiments on single-lane bus flow. *Operations Research*, 12(6):913–933, 1964.

[13] D. C. Gazis, R. Herman, and R. B. Potts. Car-following theory of steady-state traffic flow. *Operations Research*, 7(4):499–505, 1959.

[14] M. Treiber, A. Hennecke, and D. Helbing. Congested traffic states in empirical observations and microscopic simulations. *Physical Review E*, 62(2):1805, 2000.

[15] M. Bando, Hesebem K., A. Nakayama, A. Shibata, and Y. Sugiyama. Dynamical model of traffic congestion and numerical simulation. *Physical Review E*, 51(2):1035–1042, 1995.

[16] R. E. Stern, S. Cui, M. L. Delle Monache, R. Bhadani, M. Bunting, M. Churchill, N. Hamilton, R. Haulcy, H. Pohlmann, F. Wu, B. Piccoli, B. Seibold, J. Sprinkle, and D. B. Work. Dissipation of stop-and-go waves via control of autonomous vehicles: Field experiments. *Transportation Research Part C: Emerging Technologies*, 89:205 – 221, 2018.

[17] A. Talebpour and H. S. Mahmassani. Influence of connected and autonomous vehicles on traffic flow stability and throughput. *Transportation Research Part C: Emerging Technologies*, 71:143–163, 2016.

[18] R. E. Stern, Y. Chen, M. Churchill, F. Wu, M. L. Delle Monache, B. Piccoli, B. Seibold, J. Sprinkle, and D. B. Work. Quantifying air quality benefits resulting from few autonomous vehicles stabilizing traffic. *Transportation Research Part D: Transport and Environment*, 67:351–365, 2019.

[19] D. Swaroop and J.K. Hedrick. String stability of interconnected systems. *IEEE Transactions on Automatic Control*, 41(3):349–357, 1996.

[20] W. Levine and M. Athans. On the optimal error regulation of a string of moving vehicles. *IEEE Transactions on Automatic Control*, 11(3):355–361, 1966.

[21] S. Darbha and K. R. Rajagopal. Intelligent cruise control systems and traffic flow stability. *Transportation Research Part C: Emerging Technologies*, 7(6):329 – 352, 1999.

[22] B. Besselink and K. H. Johansson. String stability and a delay-based spacing policy for vehicle platoons subject to disturbances. *IEEE Transactions on Automatic Control*, 2017.

[23] M. Buehler, K. Iagnemma, and S. Singh. *The DARPA urban challenge: autonomous vehicles in city traffic*, volume 56. Springer, 2009.

[24] S. E. Shladover. Review of the state of development of advanced vehicle control systems (avcs). *Vehicle System Dynamics*, 24(6-7):551–595, 1995.

[25] R. E. Fenton and R. J. Mayhan. Automated highway studies at the Ohio State University-an overview. *IEEE transactions on Vehicular Technology*, 40(1):100–113, 1991.

[26] P. Ioannou, Z. Xu, S. Eckert, D. Clemons, and T. Sieja. Intelligent cruise control: theory and experiment. In *Proceedings of the 32nd IEEE Conference on Decision and Control*, pages 1885–1890. IEEE, 1993.

[27] R. Rajamani, S. B. Choi, B. K. Law, J. K. Hedrick, R. Prohaska, and P. Kretz. Design and experimental implementation of control for a platoon of automated vehicles. *AMSE Journal of Dynamic Systems, Measurement, and Control*, 122(3):470–476, 1998.

[28] Petros Ioannou. *Automated highway systems*. Springer Science & Business Media, 2013.

[29] V. Milanés and S. E. Shladover. Modeling cooperative and autonomous adaptive cruise control dynamic responses using experimental data. *Transportation Research Part C: Emerging Technologies*, 48:285–300, 2014.

[30] V. Milanés, S. E. Shladover, J. Spring, C. Nowakowski, H. Kawazoe, and M. Nakamura. Cooperative adaptive cruise control in real traffic situations. *IEEE Transactions on Intelligent Transportation Systems*, 15(1):296–305, 2014.

[31] L. C. Davis. Effect of adaptive cruise control systems on traffic flow. *Physical Review E*, 69(6):066110, 2004.

[32] L. C. Davis. The effects of mechanical response on the dynamics and string stability of a platoon of adaptive cruise control vehicles. *Physica A: Statistical Mechanics and its Applications*, 392(17):3798–3805, 2013.

[33] Arnab Bose and Petros A Ioannou. Analysis of traffic flow with mixed manual and semiautomated vehicles. *IEEE Transactions on Intelligent Transportation Systems*, 4(4):173–188, 2003.

[34] Arne Kesting, Martin Treiber, and Dirk Helbing. Enhanced intelligent driver model to access the impact of driving strategies on traffic capacity. *Philosophical Transactions of the Royal Society of London A: Mathematical, Physical and Engineering Sciences*, 368(1928):4585–4605, 2010.

[35] Steven E Shladover, Dongyan Su, and Xiao-Yun Lu. Impacts of cooperative adaptive cruise control on freeway traffic flow. *Transportation Research Record*, 2324(1):63–70, 2012.

[36] Bart Van Arem, Cornelie JG Van Driel, and Ruben Visser. The impact of cooperative adaptive cruise control on traffic-flow characteristics. *IEEE Transactions on Intelligent Transportation Systems*, 7(4):429–436, 2006.

[37] Anargiros I Delis, Ioannis K Nikolos, and Markos Papageorgiou. Simulation of the penetration rate effects of acc and cacc on macroscopic traffic dynamics. In *Proceedings of the 2016 IEEE 19th International Conference on Intelligent Transportation Systems (ITSC)*, pages 336–341. IEEE, 2016.

[38] G. Gunter, C. Janssen, W. Barbour, R. E. Stern, and D. B. Work. Model based string stability of adaptive cruise control systems using field data. *Submitted to IEEE Transactions on Intelligent Vehicles*, 2019, under review.

[39] G. Gunter, C. Janssen, W. Barbour, R. E. Stern, and D. B. Work. Model based string stability of adaptive cruise control systems using field data. *https://arxiv.org/abs/1902.04983*, 2019.

[40] C.-Y. Liang and H. Peng. Optimal adaptive cruise control with guaranteed string stability. *Vehicle System Dynamics*, 32(4-5):313–330, 1999.

[41] Z. Bareket, P. S Fancher, H. Peng, K. Lee, and C. A. Assaf. Methodology for assessing adaptive cruise control behavior. *IEEE Transactions on Intelligent Transportation Systems*, 4(3):123–131, 2003.